metals

MDPI

Review

Electrodeposition of Iron Triad Metal Coatings: Miles to Go

Olga Lebedeva [1], Larisa Fishgoit [1], Andrey Knyazev [1], Dmitry Kultin [1] and Leonid Kustov [1,2,3,*]

[1] Department of Chemistry, Lomonosov Moscow State University, 1-3 Leninskie Gory, Moscow 119991, Russia
[2] N.D. Zelinsky Institute of Organic Chemistry, Russian Academy of Sciences, 47 Leninsky Prospect, Moscow 119991, Russia
[3] Institute of Ecology and Engineering, National Science and Technology University "MISiS", 4 Leninsky Prospect, Moscow 119049, Russia
* Correspondence: lmkustov@mail.ru

Abstract: The possibilities and future perspectives of electrochemical deposition of bimetallic compositions and alloys containing Fe, Co, Ni, Cr, W, and Mo are reviewed. The synthesis of two- and three-component materials, as well as compositionally more complex alloys, is considered. The method of synthesizing of materials via electrodeposition from solutions containing metal ions and metalloids is one of the most promising approaches because it is fast, cheap, and it is possible to control the composition of the final product with good precision. Corrosion, catalytic and magnetic properties should be distinguished. Due to these properties, the range of applications for these alloys is very wide. The idea of a correlation between the magnetic and catalytic properties of the iron-triad metal alloys is considered. This should lead to a deeper understanding of the interplay of the properties of electrodeposited alloys. In addition to deposition from aqueous (classical) solvents, the advantages and perspectives of electrochemical deposition from ionic liquids (ILs) and deep eutectic solvents (DES) are briefly discussed. The successful use and development of this method of electrodeposition of alloys, which are quite difficult or impossible to synthesize in classical solvents, has been demonstrated and confirmed.

Keywords: electrodeposition; alloys; ionic liquids; deep eutectic solvents; coatings; functional material; nanotechnology

Citation: Lebedeva, O.; Fishgoit, L.; Knyazev, A.; Kultin, D.; Kustov, L. Electrodeposition of Iron Triad Metal Coatings: Miles to Go. *Metals* **2023**, *13*, 657. https://doi.org/10.3390/met13040657

Academic Editor: Wangping Wu

Received: 28 February 2023
Revised: 21 March 2023
Accepted: 24 March 2023
Published: 26 March 2023

1. Introduction

Various methods, such as plasma spraying, vapor deposition, magnetron sputtering and laser cladding electrodeposition, have been successfully developed for the synthesis of functionally graded material coatings (FGMC) with the composition and mechanical properties gradually changing for the optimal coating thickness. The synthesis of materials by electrodeposition (EDP) from solutions containing metal ions and metalloids and subsequently recovering alloy components is currently considered one of the most advanced techniques because it is fast, cheap, and provides the possibility of precise control of the composition of the final product. The required mechanical, corrosion, magnetic, and catalytic properties of deposited coatings are provided by varying the synthesis parameters. Electrodeposition conditions (pulse parameters, current density, electrolyte composition) can be finely tuned to control the electro-crystallization process in order to produce gradually varying composition and micro/nanostructure of the coatings [1] or amorphous coatings [2]. The electrodeposition method has been commonly used for the synthesis of FGMC due to its ease, convenience and low cost. One may find a few drawbacks to the electrodeposition process: there is a high risk of hydrogen evolution, and the inclusion of basic compounds (hydroxides) in the alloy deposits makes them powdered, stressed, or exfoliated. Some of the electrodeposition drawbacks may stem from the difficulty of co-depositing multiple elements together.

While highlighting the ability to form a smooth and homogeneous FGMC, alloys were divided into two groups: two- and three- component systems based on the metals of the iron triad with chromium or with carbon and phosphorus [3–11], and alloys containing tungsten or molybdenum. The alloy composition is chosen on the basis of its possible applications. Alloys can be applied as FGMC [12], catalysts [13], elements of micro- and nanoelectromechanical devices [14], and electrodes-electrocatalysts in the water electrolysis process [15]. The unique acid resistance and microhardness of two-component alloys based on the iron triad with Mo and W makes them an improved alternative to chromium coatings [16,17].

Ionic liquids (ILs) have already proven themselves as systems that are promising in various fields of application [18–25]. Since ionic liquids consist almost entirely of "free" charge carriers—cations and anions—their application in electrochemistry is especially interesting. The uniqueness of ionic liquids is associated with their high electrochemical stability, relatively high electrical conductivity, and the absence of a measurable saturated vapor pressure. In some cases, ionic liquids demonstrate significant advantages over traditional electrolytes. Currently, ionic liquids with an exceptionally large electrochemical window (5–9 V) have appeared, and they can be used in a cyclic mode of operation without any loss of properties or destruction of their structure, and the wide electrochemical window allows the deposition of metals with very negative redox potentials. The prospects for using ionic liquids in the processes of electrodeposition of metals and alloys and in the processes of preparation of metal and alloy nanoparticles by electrochemical methods are attractive [23,24]. ILs are good solvents for both organic and inorganic materials. ILs can be aprotic, and thus problems with regard to hydrogen ions intrinsic to protic solvents can be eliminated [25].

The review [26] considers the electrodeposition of five groups of metals (ordinary, light, noble, rare earth, and others) and their alloys in ionic liquids and deep eutectic solvents (DESs). We did not mention the preparation of nickel-phosphorus alloys and FeCoNi ternary alloys, but the properties and preparation of alloys based on nickel and cobalt are briefly described.

From a chemical point of view, ILs and DESs are two separate groups of substances to be used in the preparation of alloys. DESs exhibit several advantages over ILs, such as their easy preparation and easy availability from relatively inexpensive components (the components themselves are well-characterized in terms of their toxicity, so they can be easily shipped for large-scale processing); they are, however, in general less chemically inert. The crucial difference between ILs and deep eutectic solvents is the wide variety of ionic species present in DESs, while ILs mainly consist of one discrete type of the anion and cation [27].

The objects of this review are presented in Figure 1.

A classification of metal co-deposition based on the thermodynamic approach is proposed by Brenner [28]. In the case of "normal" co-deposition, a more noble element (having a higher equilibrium potential value) is deposited more easily, and the composition of the precipitate corresponds to the composition of the solution. "Abnormal" co-deposition can be represented by "anomalous" and "induced" behavior. Anomalous co-deposition means that less noble metals are preferably deposited. Induced co-deposition indicates that a metal that cannot be deposited in its pure form can be co-deposited as an alloy.

The fundamental aspects of co-deposition from the point of view of kinetics were developed in the work of Landolt [29]. It was proposed that the measured current density at a mixed electrode is the sum of the partial current densities of all anodic and cathodic reactions. Three types of coupling of partial reactions can be distinguished in the case of alloy deposition: non-interactive co-deposition, transport coupled co-deposition, charge transfer coupled co-deposition. These three types of coupling behavior of partial reactions during co-deposition provide a useful qualitative description of the observed behavior.

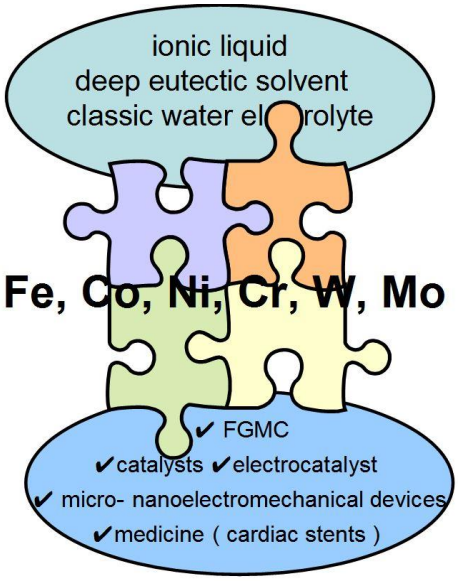

Figure 1. Bi- and ternary alloys of metals of the iron triad with chromium, molybdenum, and tungsten.

2. Electrodeposition from Water Solutions

2.1. Bi- and Ternary Alloys of Metals of the Iron Triad with Chromium and Metalloids

There are three main methods for EDP of alloys: the potentiostatic technique, direct current, and pulse current. For industrial applications, a two-electrode scheme is more suitable. For laboratory investigations, a three-electrode scheme is preferable. Schematic illustration of electroplating is presented in Figure 2.

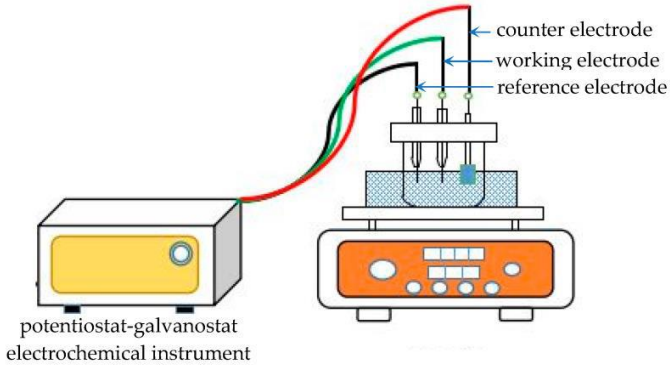

Figure 2. Schematic representation of the electrochemistry and electrodeposition experiment apparatus. Reproduced from [30] with permission from MDPI, 2023.

The most common electrodeposited materials are Ni–Fe alloy coatings [31], which, due to their remarkable electrocatalytic (reactions of hydrogen and oxygen production, CO_2 reduction), magnetic, and mechanical properties, have attracted attention in both scientific and industrial spheres. Their use in order to save Ni is economically more profitable.

Amorphous FeCr alloy films with a chromium content varying from 2.3% to 32.0 at% were deposited on a copper foil from an aqueous solution containing N,N-dimethylformamide by a potentiostatic electrodeposition technique [32]. The saturation magnetization for FeCr alloy films decreased but the microhardness increased with an increase in the chromium content.

The rate of Fe electrodeposition from the electrolytic bath is higher than that of Ni [33]. Ni-Fe coatings demonstrate unique magnetic properties.

Nanocrystalline Ni-Fe coatings were electrodeposited on steel substrates [3]. Coatings with a Fe content of 34.5% were obtained with a current efficiency of about 80%. It is

shown that Ni^{2+} and Fe^{2+} are electrodeposited together to form a single Ni_3Fe phase, and Ni deposition is inhibited by the presence of Fe^{2+}, while Fe deposition is enhanced by the presence of Ni^{2+}. The nucleation and growth of nanocrystalline NiFe coatings is an instantaneous nucleation process controlled by 3D diffusion. The average grain size is 4.8 nm, and the roughness is less than 5 nm, which is better than that of a pure Ni coating. The NiFe alloy coating demonstrates good corrosion resistance (i_{corr} = 0.7544 μA cm^{-2}, R = 8560 Ω) due to the nanocrystalline compact surface.

The magnetic field was applied simultaneously to the process of electrodeposition of Ni-Co alloy with the Co content ranging within 21.80–59.55 at% from an aqueous solution [34]. The magnetoelectrodeposited alloys exhibited high corrosion resistance in comparison with a normal electrodeposited Ni–Co coating.

The effect of ultrasonic treatment on the thermal expansion, microstructure, and mechanical properties of electrodeposited FeNi layers was studied [4]. In order to avoid high transient cavitation energy, periodic ultrasound was introduced into the electrochemical process. Periodic ultrasound weakens the stripping effect as a result of the high ultrasound power, which allows one to use both a high current density and a high ultrasound power in the electroplating process. The iron content in the electrodeposited FeNi layer increased with increasing current density. The grain size decreased with increasing the number of cycles and growing current density. With a duty cycle of 0.57 and a current density of 1 A/dm^2, a highly efficient FeNi layer with excellent surface quality is obtained (roughness = 0.95 microns; iron content = 63.00 wt.%; microhardness = 373.1 NV; Young's modulus = 133.7 MPa; coefficient of thermal expansion = 5.4 × 10^{-6}/°C). Comparative characteristics of electrodeposited NiFe alloys are given in Table 1.

Table 1. Electroplating process parameters and some characteristics of deposits.

Parameter	Ref. [3]	Ref. [4]
Electroplating process parameters		
Substrate	steel	steel
Temperature (°C)	50	55
Cathode current density (A/dm^2)	3	1
Periodic ultrasound application	no	yes
Characteristics of deposits		
Roughness (nm)	5	95
Iron content (wt.%)	34.55	63.00
Grain size (nm)	4.8	11–12

The ultrasonic treatment resulted in a sharp growth of the grain size and an increase in the surface roughness factor (Table 1), which has mostly a negative effect on the properties of the alloy. The increase in the iron content in the electrodeposited alloy is presumably associated with a four-fold higher concentration of Fe^{2+} ions in the solution (20 g/L [3] and 80 g/L [4]).

Electrodeposition offers better control over the microstructure, shape, and composition of the deposit. Ternary NiFeCo and NiFeCr alloys were deposited in aqueous solutions [35]. Both alloys exhibit superior stability as compared with their lower-order alloy and pure metal samples, with the critical temperature for grain growth (or phase decomposition) improving by nearly 100 °C in the case of NiFeCo and by 200 °C in the case of NiFeCr. Electrodeposition is a viable route towards the synthesis of strong and highly stable nanocrystalline medium-entropy alloys (MEAs, containing 3–4 elements). The electrocatalytic activity in the hydrogen evolution reaction (HER) and oxygen evolution reaction (OER) in alkaline media for ternary nanostructured NiFeCo coatings and binary coatings electrodeposited in aqueous solutions was compared [36]. The comparison of the electrocatalytic activities of electrodeposited crystalline NiFeCo and amorphous NiFeCoP in HER showed the superior properties of NiFeCoP [37]. The authors [36,37]

explain the high electrocatalytic activity by more developed surface and the synergy of the alloy components.

The electrochemical formation of Cr-C coatings was also studied [5]. The electrochemical formation of Cr-C coatings is realized through the simultaneous reduction of Cr(III) and decomposition of an organic ligand. The chemical state of metalloids (for example, carbon, phosphorous, and boron) in coatings electrodeposited from Cr(III) solutions may be determined with Valence-to-Core X-ray Emission spectra (vtc-XES, vtc-X-ray). The vtc X–ray spectra allowed one to determine the presence of metalloid atoms that are covalently bound to metal atoms and to estimate their quantitative content in metal-metalloid coatings formed by various methods (Figure 3).

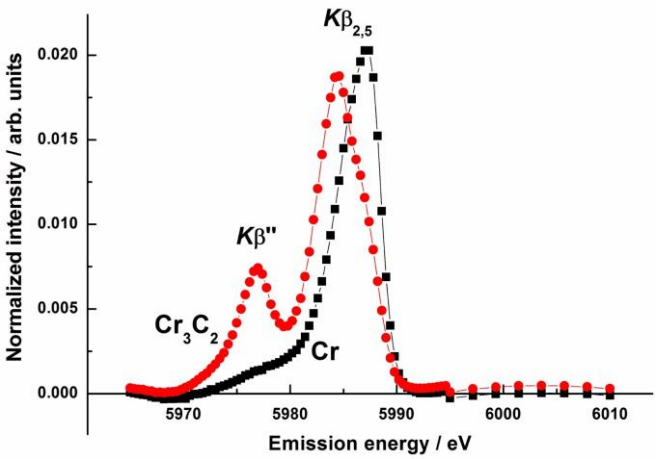

Figure 3. Normalized vtc X–ray emission spectra of metallic chromium and Cr3C2 carbide used in modeling experimental spectra of vtc X-ray of Cr–C samples. Reproduced from [5] with permission from Elsevier, 2018.

The comparison of vtc X–ray data with data on the total amount of carbon in the samples obtained, for example, by X-ray diffraction makes it possible to divide the total amount of carbon in the samples by the amount of elemental carbon and carbon that is covalently bound to chromium atoms. It should also be noted that for the obtained coatings with a carbon content below 40 at.%, an increase in the size of crystallites was observed after calcination at 500 °C. Coatings with a high carbon content do not show any signs of long-range order in their crystal structure.

Electrodeposition of metal–metalloid alloys of the NiP type was considered [6,7]. The effect of heat treatment and variation of the phosphorus content on the magnetic properties of electrodeposited NiP alloys was investigated [6]. The magnetic properties of the alloys obtained were explained with the use of differential scanning calorimetry (DSC) data. Magnetization measurements and DSC analysis of NiP alloys showed that the alloys with a phosphorus content exceeding 12 at.% were paramagnetic due to the absence of exchange interaction as a result of the formation of a network of P–rich paramagnetic domains. Amorphous NiP alloys, which were originally paramagnetic, became ferromagnetic after the heat treatment, which also led to their devitrification. The transition to the ferromagnetic state occurred as a result of the formation of the ferromagnetic phase of nickel, while the coercive force of the alloy increased due to an increase in the crystallite size and an increase in the proportion of the paramagnetic phase (Figure 4).

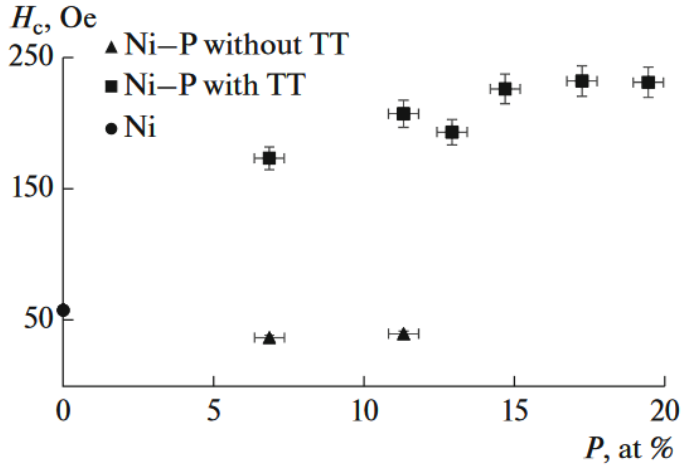

Figure 4. Effect of the phosphorus content on the coercive force of Ni–P coatings in the initial state and after thermal treatment relative to the coercive force of pure nickel. Reproduced from [7] with permission from Pleades Publ., 2017.

Regardless of the heat treatment, the magnetization of the alloys and the saturation magnetization decreased with increasing phosphorus content in the alloy.

Electrodeposition of Ni-P coatings was performed from an aqueous solution by direct current using a stirring time-controlled technique. Stirring leads to the formation of Ni-P layers with a higher P content, while without stirring Ni-P layers with a lower P content are produced [38].

The composition of NiP alloys depends on the content of sodium hypophosphite in the electrolyte in the course of the electrochemical deposition of an amorphous nickel coating. It was found for the first time [7] that alloys obtained under similar deposition conditions from electrolytes with fixed concentrations of nickel sulfate and sodium citrate have phosphorus concentrations ranging from 0 to 22–23 at.%. The Curie temperature of the obtained Ni–P samples, which are ferromagnetic in their initial state ([P] < 12 at.%), is in the range of 150–200 °C. At the same time, all heat-treated Ni–P samples demonstrated a Curie temperature close to that of pure nickel in the range of 350–360°C. The initial electrodeposited alloys become paramagnetic when they contain phosphorus in concentrations higher than 12 at.%. It is due to the lack of the possibility of exchange interaction as a result of fluctuations in the chemical composition. Paramagnetic alloys of the NiP type, after heat treatment, which leads to their uncovering, exhibit ferromagnetic properties due to the release of the ferromagnetic phase of Ni. An increase in the phosphorus concentration leads to an increase in the coercive force as a result of an increase in the grain size and in the proportion of the paramagnetic phase. The residual magnetization and saturation magnetization of alloys decrease with the increasing phosphorus concentration in the case of both heat-treated and non-heat-treated alloys.

The results of these works [6,7] could serve as a basis for theoretical predictions and systematic and rational analysis of various factors affecting the magnetic properties of materials containing several ferromagnetic elements.

The mechanism of electrochemical deposition of NiCrP alloys in a glycine bath was studied [8]. Electrodeposition on a copper plate was carried out at a current density of 10–20 A/dm^2. The electroreduction mechanisms of individual Cr and Ni, NiCr, NiP, CrP, and NiCrP alloys were studied. The possible process of trivalent chromium reduction can be explained by the formation of a glycine complex of bivalent chromium $[Cr(H_2O)_4(Gly)]^+$ (Equation (1)). The bivalent chromium complex was directly reduced to metallic chromium (Equation (2)). The reduction process of nickel is described by Equation (3). The key to NiCr co-deposition is the ΔE value for the reduction of nickel and chromium ions. During electrodeposition of the NiCr alloy, nickel is initially deposited on the surface of the cathode (Equation (3)). Nickel acts as a catalyst, causing a significant positive shift in the initial

reduction potential of Cr(II) ions, thus satisfying the potential difference (approximately −180 mV) for the co–deposition of NiCr.

Nevertheless, the actual potential difference between Ni and Cr is the same as in the case of NiCr co–deposition, which ensures electrodeposition of the three–component alloy for the NiCrP system. In addition, it has been demonstrated that P tends to co-precipitate with Cr during the electrodeposition of NiCrP, which can be explained by the difference in the behavior during the electrodeposition of NiP and CrP alloys. The possible reduction processes can be presented as follows:

$$[Cr(H_2O)_4(Gly)]^{2+} + 1\ e = [Cr(H_2O)_4(Gly)]^{+} \quad (1)$$

$$[Cr(H_2O)_4(Gly)]^{+} + 1\ e = Cr^0 + Gly + 4H_2O \quad (2)$$

$$Ni^{2+} + Ni^{+}{}_{ads} + 2\ e = Ni^0 + Ni^{+}{}_{ads} \quad (3)$$

The possible mechanism of Ni–P electrodeposition can be explained as follows (Equations (4) and (5)):

$$H_2PO_2{}^{-} + 5H^{+} + 4\ e = PH_3 + 2H_2O \quad (4)$$

$$2PH_3 + 3Ni^{2+} = 3Ni^0 + 2P + 6H^{+} \quad (5)$$

The inorganic complexing agent used to obtain a CrP alloy is $NaH_2PO_2{\cdot}H_2O$. The P incorporation mechanism in the course of the CrP alloy deposition is considered to be different from that realized in the case of the NiP alloy deposition.

The techniques used to produce multilayer and gradient coatings have been demonstrated in a review [39]. Ni-W multilayers were produced by varying the direct current density. Comparison of the direct and pulse currents on the properties of deposits was performed. The technique controlling the electrode potential is also effective for multilayer coating production. Metals of the Fe-triad are commonly used in multilayer coatings electrodeposited by controlling the electrode potential. The necessity of studying the electrode kinetics and the effects of various additives is shown.

So, a trivalent chromium solution containing glycine and $NaH_2PO_2{\cdot}H_2O$ may also form a complex with hypophosphite, i.e., the $[Cr(H_2PO_2)(H_2O)_5]^{2+}$ complex. Taking this into account, the positive shift in the onset potential of CrP codeposition is associated with the increase in the concentration of electroactive Cr(III) complexes near the cathode (Equations (6)–(8)):

$$[Cr(H_2PO_2)_4(H_2O)_5]^{2+} + 1\ e = [Cr(H_2PO_2)_4(H_2O)_5]^{+} \quad (6)$$

$$[Cr(H_2PO_2)_4(H_2O)_5]^{+} + 2\ e = Cr^0 + 5H_2O + H_2PO_2{}^{-} \quad (7)$$

$$3H_2PO_2{}^{-} = H_2PO_3{}^{-} + 2P + H_2O + 2OH^{-} \quad (8)$$

The XRD analysis showed that the electrodeposited alloy coatings had an amorphous structure. The incorporation of phosphorus in the Ni deposit generally increases the number of defects in the crystalline lattice of electrodeposited alloy coatings, thereby transforming the coatings from a crystalline to an amorphous state. Scanning electron microscope images showed that a smooth and compact NiCrP coating was obtained at a current density below 15 A/dm^2 (Figure 5).

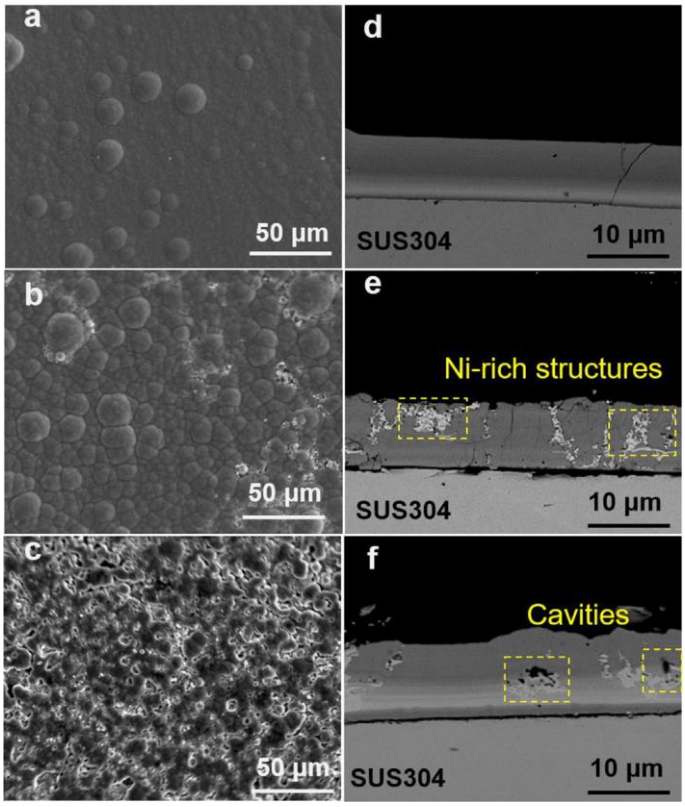

Figure 5. SEM micrographs of the surface (**a**–**c**) and cross-sectional micrographs (**d**–**f**) of coatings prepared from electrodeposited NiCrP alloys at the current densities (**a**,**d**) 10 A/dm^2, (**b**,**e**) 15 A/dm^2, (**c**,**f**) 20 A/dm^2. Reproduced from [8] with permission from Elsevier, 2021.

Electrodeposited NiCoP, FeCoP, and FeNiP alloys have been prepared [9–11]. The authors [9] applied magnetic assisted jet electrodeposition for effectively changing the microstructure and properties of NiCoP alloy films. The advantage of this method is inhibition of the growth of pores on the surface of the film and improving the adhesion of the coating to the surface. An increase in the saturation magnetization of the coating was observed as compared with simple jet electrodeposition.

The effect of calcination on the structure of coatings is analyzed using a combination of vtc-XES and X-ray diffraction to conclude whether recrystallization involves any redistribution of covalently bound metalloid between atoms of different metals in a three-component system [10,11]. The NiCoP, FeCoP, and FeNiP alloys were electrodeposited on a copper substrate from solutions containing Fe(II), Co(II), and Ni(II) with NaH_2PO_2 additives were taken as the object of the study. The FeNiP system was described in detail in ref. [10].

The corrosive and mechanical properties of cobalt-nickel-phosphorus ternary alloy coatings are discussed [40]. The role of pH, bath composition, and conditions of electrodeposition are summarized.

The vtc-XES data show that the coatings contain a high concentration of chemically bound phosphorus. Comparison of the vtc-XES spectra of all initial and calcined coatings [10,11] allows one to unequivocally conclude that the concentration of chemically bound phosphorus changes slightly due to crystallization, as for the two-phase electrodeposited alloys described above [6,7].

2.2. Iron Triad Metal Alloys with Molybdenum and Tungsten

Nickel-molybdenum alloys are promising electrocatalysts for HER. There are two main methods for EDP of NiMo alloys, namely, electrodeposition by direct current and by the pulsed current [40–43]. The method of EDP by pulsed current is preferable since it allows one to apply also the duty cycle or effective time of the applied current.

The relationship between independent variables and coating properties was established. In particular, the effect of nickel sulfate and sodium/molybdenum concentrations on various electroplating reactions was evaluated. Coatings with a high percentage of Mo and distinct morphology were obtained. X-ray diffractograms showed that all the samples were amorphous. The optimal bath composition was found at the ratio Ni:Mo of 7.5:5. A film with a maximum Mo content of 29 wt.% was obtained. However, the alloy with the best corrosion properties was deposited from a bath with a Ni:Mo component ratio of 10:3. The NiMo alloys were deposited by the pulsed current [42]. The morphology of the samples and the Mo content in the alloys were affected by a change in the working cycle from 70% to 30%. The material exhibited a crystalline structure. All the analyzed NiMo alloys showed activation of the hydrogen release reaction at a 30% duty cycle. The mechanism of the electrodeposition was proposed based on the published results [44–47].

The corrosive, mechanical, and magnetic properties of alloys containing metals of the iron group with tungsten are highlighted in a review [48]. Modern codeposition mechanisms are critically discussed.

The two-component alloys of the NiW and CoMo types were electrodeposited on a Cu substrate by the direct current method [49]. The deposition of the CoMo composition was carried out at i = 30–120 mA/cm^2, t = 10–60 min, T = 298 K, pH = 5.0–9.0. The alloy composition (wt.%) was determined by EDX: O(2–10), Co(13–87), Cu(0.7–7.6), Mo(7–50). All samples are characterized by a small coating thickness (less than 30 microns) and by the presence of copper in the alloy, which makes them translucent from the substrate. The presence of oxygen (up to 10 wt.%) in the composition of the electrodeposited coating indicates the products of incomplete reduction, i.e., oxide phases. The surface quality of alloys with a sufficient amount of Mo is bad. Cracks can be seen as a result of accumulated micro stresses and possible formation of hydrogen clusters, also described elsewhere [50,51]. Summing up the mechanism of the joint electrodeposition of cobalt and molybdenum according to the results available in the literature [46,52,53], it can be stated in the simplest version as follows: initially, metallic cobalt is electrodeposited on the cathode, a thin layer of which acts as a catalyst for the reduction of molybdenum ions with hydrogen. The formation of a joint complex of molybdenum and a precipitating metal contributes to the transfer of charges to the molybdenum ion through the precipitating metal. Molybdenum co-precipitates with metals of the iron triad due to the energy gain caused by alloying. The electrolyte containing sodium pyrophosphate as a complexing agent turned out to be more effective than a citrate-containing agent in terms of forming thicker coatings, however, no sample had sufficient thickness to study it by X–ray phase analysis, therefore, the approximate phase composition of the samples can be judged by the nickel-molybdenum state diagram. The deposits are basically formed in the two-phase region Mo_6Co_7+$MoCo_3$. The deposition of the NiW system was carried out at I = 80–300 mA/cm^2, t = 30 min, T = 298 K. The alloy composition (wt.%) was determined by EDX: O(5–13), Ni(13–85), Cu(6–18), W(3–15). The deposits obtained at the maximum cathode current density demonstrated relatively low oxygen contents. The copper content in the alloy decreases with an increase in the cathode current density. The nickel content in the alloys increases with an increase in the current density.

The content of tungsten in the coatings increases with an increase in the concentration of tungstate ions in the solution and does not depend on the current density. The optimal composition is achieved in alloys obtained from the most concentrated solutions of tungstic acid salts at maximum current densities. Authors [51] proposed that non-electrochemical deposition of tungsten in the form of oxides was observed.

According to the Brenner classification, deposition of nickel-tungsten alloys is conducted in the form of "induced co-deposition". The joint electrodeposition of tungsten and nickel is divided into four main stages [54–57]:

1. Electrochemical generation of reactive forms of nickel and tungsten. The intermediate forms of these metals with an unpaired electron, i.e., particles of the radical type, exhibit a particularly high reactivity;

2. Formation of refractory metals from reactive particles of heteropoly compounds due to electrode initiation of the polymerization process. The film formed in this case has a low electron conductivity;
3. Electrochemical reduction of metal ions in the non-metallic system at the point of contact of parts of the film with ions in different oxidized states;
4. Final electrochemical reduction of metal ions at the film-alloy interface.

The alloy formation model will be valid if the film has low electron conductivity. Only in this case is a high negative potential achieved at the alloy-film boundary, and the release of hydrogen is blocked since the removal of gaseous hydrogen is very difficult. Consequently, the alloy is obtained at the film-alloy boundary by the following total reaction [55]:

$$[(Ni)(WO_4)(Cit)(H)]^{2-} + 8e- + 3H_2O \rightarrow NiW + 7(OH)^- + Cit^{3-} \quad (9)$$

The presence of copper in deposits indicates a thin coating, and the excess of oxygen can be explained by the fact that the deposition of tungsten occurs in the form of tungsten blue $WO_{3n}(OH)_n$ ($0.1 \leq n \leq 0.5$).

Ternary alloys CoNiW were electrodeposited on a copper substrate by using a direct or pulsed current were studied [50,51,58,59]. The content of each element in the coating was in the range of 5–35 at.%, which corresponded to the definition of a high-entropy alloy [50]. A crack-free coating can be obtained by applying a pulsed current with an average current density of 15 mA/cm^2. All coatings obtained under various electrodeposition conditions had an amorphous structure, which indicated the formation of a solid solution on the substrate. Cracks, usually caused by internal stress or hydrogen embrittlement, can be observed on coatings obtained by the direct current method. The corrosion potentials of the coatings were lower than those of the substrate, but the corrosion current density decreased. The coating can increase the Cu substrate protection efficiency up to 73.8%. The influence of the bath composition and electrodeposition parameters on the structure, composition, surface characteristics and corrosion properties of NiWCo alloys was investigated [51]. Corrosion and wear characteristics were evaluated. It has been proved that the CoNiW alloy has a homogeneous, compact and flat surface exhibiting a colony-like morphology. An amorphous or nanocrystalline structure was formed depending on the process parameters, including the current density, pH, and electrolyte composition. The size of the crystallites did not depend notably on the Co content, but strongly depended on the current, pH of the solution and the synthesis time. The average roughness was optimized to 4–7 nm. The triple alloy contains 33 wt.% W, 21–60 wt.% Ni, and 2.8–40 wt.% Co. A decrease in the nickel content in deposits corresponds to an increase in the Co content. The W content somewhat changed while varying the electrodeposition conditions. The intermediates for the formation of the CoNiW alloy are $[Ni(HWO_4)(C_6H_5O_7)]^{2-}$ and $[Co(HWO_4)(C_6H_5O_7)]^{2-}$ ions. The addition of alumina nanoparticles slightly increases microhardness, reduces adhesive and oxidative wear, and significantly increases wear resistance [59]. The way that coatings wear out depends on the conditions of deposition. Alloys of the CoNiW type with a composition and structure gradually changing in thickness were synthesized using direct current electrodeposition [58–60]. A simple and convenient method of synthesis by induced electrodeposition is applicable to obtain multicomponent functional coatings [58].

Solution plasma sputtering is a simple and facile technique for the synthesis of NPs in a solution [61]. A schematic diagram demonstrates the formation of nanoparticles via the plasma sputtering method (Figure 6).

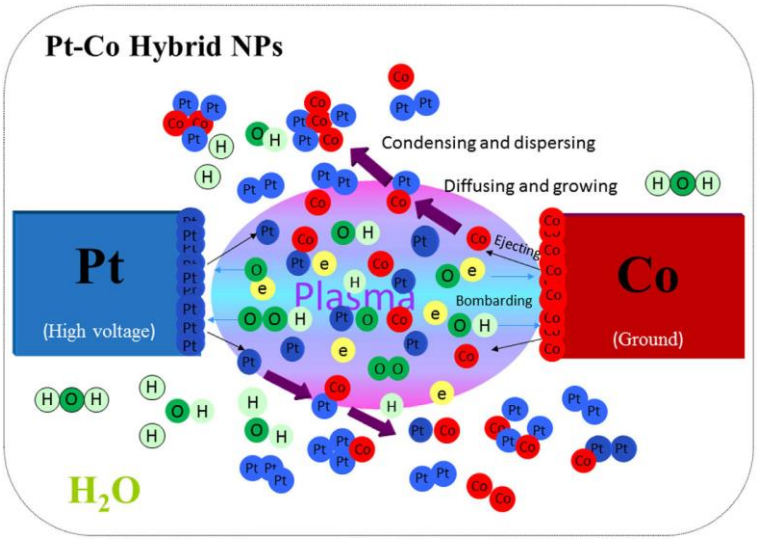

Figure 6. Schematic diagram for the synthesis of Pt/CoPt-1 composite NPs by solution plasma sputtering. Reproduced from [61] with permission from Nature, 2017.

The plasma generation technique in the liquid phase was used to synthesize alloy NPs with unique properties suitable for many applications [62].

3. Electrodeposition of Two- and Three-Component Alloys in Ionic Liquids and Deep Eutectic Solvents

3.1. Electrodeposition of Alloys in Ionic Liquids

The comparison of aqueous solutions and organic solvents with ionic liquids (ILs) as electrolytes is presented in the literature [63,64]. Some ionic liquids are manufactured on a commercial scale. The use of ILs in the electrodeposition of metals and alloys results in enhanced current efficiencies (CE > 90%) and production of corrosion-resistant and non-flaking coatings. The use of ILs in electrodeposition may be realized by three manners:

i. "pure" ILs
ii. ILs with additives [65]
iii. ILs as additives [66]

As received "pure" ILs may contain different impurities, mostly water. Such substances as acetonitrile, coumarin, thiourea, benzotriazole, acetone etc., are commonly considered as additives. By replacing some of the bulky adsorbed IL cations, the additive molecules can induce a more facile electrode reaction. As a consequence, a smoother and shinier surface is obtained in the presence of additives [65,67].

The electrodeposition of a Ni-Fe alloy from DES with water additives was studied [68]. The authors found that "abnormal" co-deposition occurs in the presence of water.

Ni-Co alloys were deposited from aqueous solutions with different metal salts and with additives of ILs 1-methyl-3-(2-oxo-2-((2,4,5-trifluorophenyl)amino)ethyl)-1H-imidazol-3-ium iodide ([MOFIM]I) and 1-(4-fluorobenzyl)-3-(4-phenoxybutyl)imidazol-3-ium bromide ([FPIM]Br) [66]. It was shown that the composition of alloys depended on the composition of the electrolyte (Table 2).

Table 2. The content of Co^{2+} in the electrolytic solution (wt.%) and the cobalt content (at.%) in the deposited Ni-Co alloys without and with additives.

Composition	Cobalt Content		
Composition of the electrolytic solution	30	50	70
Composition of deposited alloy			
1. without ILs	38.03	59.8	79.0
2. with [MOFIM]I	35.9	65.65.	85.33
3. with ([FPIM]Br	48.96	60.76	83.62

Electrodeposition of a Ni-Co alloy onto a Cu substrate was performed using an acidic sulfate bath in the absence and presence of different concentrations of [MOFIM]I and [FPIM]Br [19]. The corrosion behavior of coelectrodeposited Ni-Co alloys was performed in a marine water medium. A higher extent of inhibition of Ni^{2+} and Co^{2+} reduction is indicated by the increasing shift of the cathodic polarization curves towards more negative potentials (Figure 7).

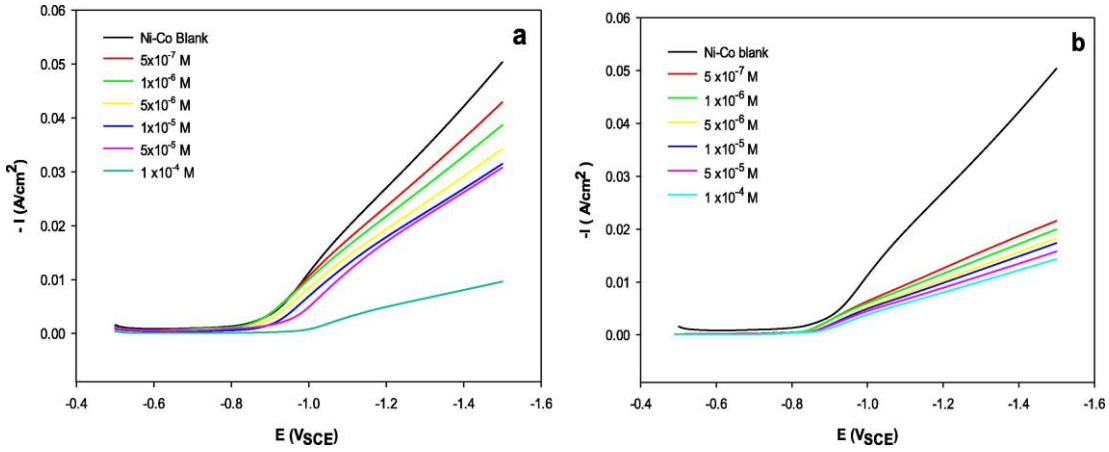

Figure 7. Potentiodynamic cathodic polarization curves for the Ni-Co alloy electrodeposition from the Ni70%-Co30% bath in the absence and presence of different concentrations of (**a**) [MOFIM]I, (**b**) [FPIM]Br at pH 4.5. Reproduced from [19] with permission from Elsevier, 2021.

The inhibition effect of the [MOFIM]I and [FPIM]Br molecules due to their adsorption on the cathode surface obeys the Langmuir adsorption isotherm. Compared with [FPIM]Br, [MOFIM]I reveals a better corrosion inhibition efficiency and more efficient additive properties. According to the natural atomic charges, [MOFIM]I demonstrates the strongest adsorption ability on the Cu substrate and a higher IE_Rct% compared with [FPIM]Br. These results show that the theoretical results are consistent with the experimental findings.

The study [20] shows the possibility of electroplating the surfaces of Fe, Ni, and Ni-Fe in ionic liquids as solvents without hydrogen evolution. It is important to remark that Ni-Fe alloy electrodeposition was successful in 1-butyl-1methylpyrrolidinium bis trifluoromethylsulfonyl)imide ([P1,4][Tf2N]) even though iron films are difficult to plate alone. An unexpected change of the alloy composition versus polarization (increase, decrease and further increase in the iron atomic percentage) was observed.

A summary of the recent literature discussing the use of ILs in the preparation of electrocatalysts based on Ni-alloys for OER and HER was presented [21]. It was shown in the review how ILs function as solvents and electrolytes for high-temperature electrodeposition baths, as well as structure-directing agents, doping agents, stabilizers, and/or capping agents in nanoparticle synthesis. For example, the mechanism for the synthesis of Ni2P nanoparticles from the tetrabutylphosphonium chloride ([P4444]Cl) ionic liquid was proposed (Figure 8).

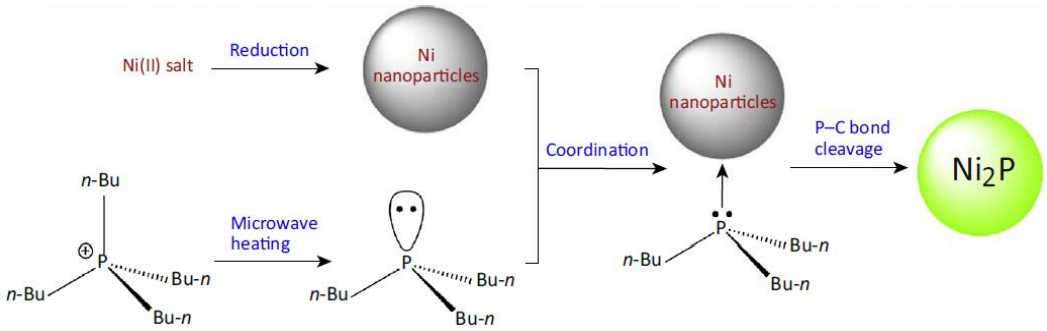

Figure 8. The mechanism for the synthesis of Ni2P nanoparticles from the [P4444]Cl ionic liquid. Reproduced from [19] with permission from Elsevier, 2021.

The IL was found to be the source of phosphorus in the resulting nickel phosphides through a suggested mechanism involving decomposition under heating to generate tributylphosphine, coordination of tributylphosphine with Ni(0) nanoparticles, and subsequent cleavage of the remaining P–C bonds as shown in Figure 8 (i.e., capping and doping). Understanding the role of the structure of the double electric layer of IL in electrochemical processes, in particular in the electrodeposition of metals and alloys, will allow one to predict the conditions for obtaining deposits with the desired properties [69].

So, the use of IL in industry is still at the very early stage [64]. The authors [21] stressed that often it is not obvious why a given IL is selected for a chosen task. The major drivers for industrial use of ILs are their cost and availability. The other reason for the restriction on the commercialization of some ILs is their toxicity (imidazolium-based ILs). The major limitations for industrial electrodeposition of metals and alloys in ILs are [63]:

- The relationship between the precipitate structure and the composition of the IL has not been studied in detail yet;
- Coatings must achieve quality standards, and process development is required to a large extent;
- Some applications are at the fundamental research stage with associated higher risk, that is, electroless, semiconductor, anodizing, and nanocomposite coatings;
- Process economics has been determined for a limited number of processes.

Only when these problems are properly solved will the full potential of these unique solvents in the production of efficient electrodeposited electrocatalytic materials be realized.

3.2. Electrodeposition in Deep Eutectic Solvents (DESs)

DESs based on choline chloride (ChCl) and other quaternary ammonium salts are most often applied for the deposition of metals and alloys [15,27]. Examples of compounds forming deep eutectic solvents (DES) with ChCl are anhydrous and crystal hydrates of metal salts, urea, ethylene glycol (EG), and many others. Chromium precipitation from aqueous solutions occurs with a rather low current efficiency and is accompanied by precipitation of basic compounds (salts, hydroxides). The inclusion of the latter in the precipitate led to the formation of powdered, strained, or flaking precipitates [70]. DESs usage let one to obtain dense precipitates with greater adhesion.

According to Abbot [71], DES is promising for obtaining coatings with new compositions and unique properties. The review discusses the effect of additives (especially water) on the electrodeposition of metals and alloys from DES. Water changes the structure of the double electric layer and improves mass transfer [71]. The electrodeposition of a Ni-Fe alloy from DES with water additives (up to 15 wt%) was studied [68]. The authors found that "abnormal" co-deposition occurs in the presence of water. The review by Smith [72] noted that, despite the fact that DES is economically difficult to compete with aqueous electrolytes, they may be of some value for industrial applications.

Nanoscale Fe-Cr alloy was successfully electrodeposited in a choline chloride-ethylene glycol (ChCl-EG, mole ratio 1:3) deep eutectic solvent in a two-electrode system by optimiz-

ing the concentration ratio $C_{Fe(II)}/C_{Cr(III)}$ [18]. ESI-MS analyses indicate that $[Fe(H2O)_3(Cl)_3]^-$ and $[Cr(H_2O)_2Cl_4]^-$ are the dominant species of Fe(II) and Cr(III) in ChCl-EG DES, respectively. Linear sweep voltammetry demonstrates that with the increase in $C_{Fe(II)}/C_{Cr\ (III)}$ from 1:5 to 1:1, the reduction potential difference between Fe(II) and Cr(III) becomes smaller, which is conducive to the electrodeposition of a Fe-Cr alloy deposit with a higher Cr content. The reduction of Fe(II) or Cr(III) on a glassy carbon electrode is a quasi-reversible process controlled by diffusion, with diffusion coefficients of $5.34 \cdot 10^6$ cm^2/s and $2.22 \cdot 10^6$ cm^2/s, respectively. FE-SEM observation shows that as the $C_{Fe(II)}/C_{Cr\ (III)}$ ratio decreases from 1:2 to 1:5, the microstructure becomes non-uniform, and the morphology transforms from homogeneous particles to scaly blocks. At the ratio of 1:2, the prepared nanocrystalline Fe-Cr alloy exhibits a symmetrical element distribution with a mean coating thickness of 120.3 μm and a mean diameter of 1.56 nm (Figure 9). Good corrosion resistance was revealed for the prepared Fe-Cr alloy. All the above studies provide a theoretical foundation for Fe-Cr alloy production by varying the electrolyte ratios.

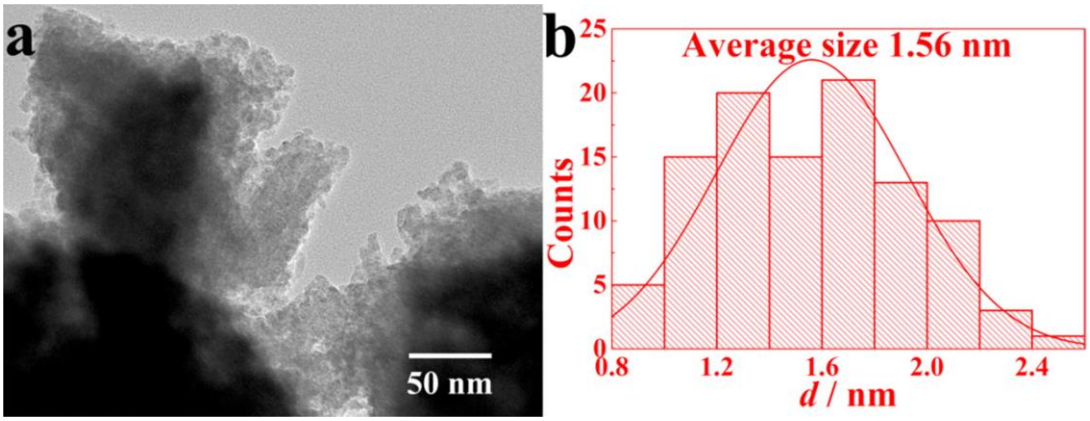

Figure 9. Fe-Cr alloy synthesized at the concentration ratio $c_{Fe(II)}/c_{Cr(III)}$ of 1:2 in ChCl-EG DES. (**a**) TEM image; (**b**) The particle size histogram. T = 333 K; U = 2.8 V. Reproduced from [18] with permission from Elsevier, 2022.

Ni-Co coating was deposited from DES by a potentiostatic technique on glassy carbon and Si/Ti/Au electrodes [73]. The CoNi films presented two CoNi alloyed crystal structures; therefore, the formation of Ni cubic crystalline structures and amorphous Co nanocrystalline structures was promoted. The deposits were tested as platforms to activate the formation of sulfate radicals.

The effects of the deposition potential on the morphology, chemical composition, crystal structure, corrosion resistance, and magnetic properties of nanostructured Fe-Co-Ni coatings were investigated [22]. The Fe-Co-Ni coatings prepared from ChCl/2Urea DES at different deposition potentials showed good corrosion resistance. Fe-Co-Ni coating that is produced at the deposition potential of −1.2 V (vs. saturated calomel reference electrode), exhibited a more positive corrosion potential and obvious magnetic anisotropy. The effective electrodeposition of nanostructured Co-films with a high surface area was performed by DES [74].

The coatings with the Fe contents of 89, 69, 47, and 28 at% were electrodeposited from DES [75]. The electrocatalyst with 69% Fe demonstrated high activity in HRR in alkaline media. The comparison of the alloy and the bath composition showed a close match.

The Fe and Fe-Ni coatings were electrodeposited in novel DES consisted of mixtures of $FeCl_3$ (or $NiCl_2$) and acetamide [76]. The Fe–Ni alloys demonstrated high corrosion resistance. The 1:1:10 $FeCl_3$–$NiCl_2$–acetamide mixture produced three deposits with compositions: Fe and alloys Fe72Ni28 and Fe12Ni88.

NiMo alloys were obtained from DES by the pulsed technique [42] at potentials ranging from −0.5 to −0.9 V vs. Ag [77] and with the conventional Watts bath [78].

Ni–P alloy coatings with tunable phosphorus contents are electrodeposited onto a platinum electrode at room temperature using choline chloride, ethylene glycol (1:2 molar ratio) as a deep eutectic solvent, and $NiCl_2 \cdot 6H_2O$, $NaH_2PO_2 \cdot H_2O$ as nickel and phosphorus sources, respectively. Cyclic voltammetry shows that the presence of $H_2PO_2^-$ in the ionic liquid in the case of Ni plating promotes the initiation of Ni–P nucleation [79]. The structure of Ni–P deposits is converted from a crystalline to an amorphous structure with the increase in phosphorus content in the coating.

There is no unambiguous opinion regarding the use of DES for the electrodeposition of metals and alloys [15,71,72]. At present, the comparison of industrial production of functional materials in DES and in aqueous solutions is not in favor of the former. From a practical point of view, DESs application for the deposition of coatings based on most of the metals (iron, copper, brass, nickel, and their alloys) used in the industry to produce functional materials is yet not realistic [15,72]. However, in the future, the use of DES as an electrolytic medium may open up opportunities for obtaining alloys of new compositions with unique physicochemical properties [71].

The main advantages and disadvantages of water and anhydrous electrolytes for metal electrodeposition can be summarized on the basis of the analysis of literature data (Table 3).

Table 3. Main advantages and disadvantages of classic (water) and modern electrolytes for electrodeposition.

Electrolyte	Advantages	Disadvantages	Ref.
Classic water solutions	low temperature, low cost, fast, good adhesion of deposit, easy to control thickness of the deposit, wide range of metal salt concentration	pH dependent, low current efficiency and porosity due to hydrogen evolution. High concentration of toxic component, the anion formation in the solvent decomposition process can lead to the occurrence of a precipitation with the metal ion	[26,70]
ILs	pH independent, deposition metals that are not accessible with conventional aqueous solution, good solvent for organic and inorganic substances	High cost, toxic, different impurities (water et al.)	[3,4,25]
DES	Deposition metals that are not accessible with conventional aqueous solution, the anion formation in the solvent decomposition process can not lead to the occurrence of a precipitation with the metal ion, low cost, non toxic, easy preparation, high purity	There are few systematic studies	[15,20,23]

4. Conclusions

- The relevance of electrodeposited alloys with a wide range of useful properties, such as corrosive, electrocatalytic, and magnetic properties, is shown. Due to these properties, the scope of applications for these alloys is very wide. The ability to deposit alloys on parts of a complex shape increases the wear and corrosion resistance of the latter.
- It is very important to study the correlation between the concentration of metal ions in the electrolytic bath and the metal content in the reduced form to describe the technique of manufacturing the coatings.
- Also promising, in our opinion, will be the establishment of a correlation between the magnetic and catalytic properties of electrodeposited alloys based on iron triad metals. Another promising direction of research on the properties of electrodeposited nickel- and cobalt-based alloys with modifying additives is the use of these materials in medicine, for example, as a replacement for platinum cardiac stents [61–64].
- The potentiostatic, ultrasonic, and plasma generation techniques in liquid are promising approaches in the electrodeposition process. Solution plasma sputtering is a simple

and facile technique for the preparation of highly dispersed nanomaterials (metals and alloys) on a variety of carriers, such as metal oxides and carbon materials.

- The electrochemical deposition of alloys based on Fe-triad with aqueous (classical) solvents due to their advantages (Table 3) is today the most commonly used technology for industry. Due to their specific physicochemical and electrochemical properties, ionic liquids and DES are promising for obtaining coatings with new compositions and unique properties that cannot be obtained from classical solvents.

Author Contributions: O.L.—writing and draft preparation of all Parts; and final version preparation; L.F.—writing and draft preparation of Parts 1,2; A.K.—writing and draft preparation of Parts 2; D.K.—writing and draft preparation of Parts 1,3; and final version preparation; L.K.—editing and proof-reading, and final version preparation. All authors have read and agreed to the published version of the manuscript.

Funding: This work was supported by the Ministry of Science and Higher Education of the Russian Federation (grant no. 075-15-2021-591).

Informed Consent Statement: Not applicable.

Data Availability Statement: Not applicable.

Conflicts of Interest: The authors declare no conflict of interest.

Abbreviations

ionic liquids (ILs), deep eutectic solvents (DES), functionally graded coatings (FGC), hydrogen evolution reaction (HER), oxygen evolution reaction (OER), from differential scanning calorimetry (DSC), X-ray emission spectroscopy (vtc-XES), high-entropy alloy (HEA), direct current (DC), pulse current (PC), choline chloride (ChCl), ethylene glycol (EG).

References

1. Zangari, G. Electrodeposition of Alloys and Compounds in the Era of Microelectronics and Energy Conversion Technology. *Coatings* **2015**, *5*, 195–218. [CrossRef]
2. Ma, L.; Xiaoli, X.; Nie, Z.; Dong, T.; Mao, Y. Electrodeposition and Characterization of Co-W Alloy from Regenerated Tungsten Salt. *Int. J. Electrochem. Sci.* **2017**, *12*, 1034–1051. [CrossRef]
3. Li, Y.; Cai, X.; Zhang, G.; Xu, C.; Guo, W.; An, M. Optimization of Electrodeposition Nanocrytalline Ni-Fe Alloy Coatings for the Replacement of Ni Coatings. *J. Alloys Compd.* **2022**, *903*, 163761. [CrossRef]
4. Li, A.; Zhu, Z.; Xue, Z.; Liu, Y. Periodic Ultrasound-Assisted Electrodeposition of Fe–Ni Alloy Foil. *Mater. Res. Bull.* **2022**, *150*, 111778. [CrossRef]
5. Safonov, V.A.; Habazaki, H.; Glatzel, P.; Fishgoit, L.A.; Drozhzhin, O.A.; Lafuerza, S.; Safonova, O.V. Application of Valence-to-Core X-Ray Emission Spectroscopy for Identification and Estimation of Amount of Carbon Covalently Bonded to Chromium in Amorphous Cr-C Coatings Prepared by Magnetron Sputtering. *Appl. Surf. Sci.* **2018**, *427*, 566–572. [CrossRef]
6. Knyazev, A.V.; Fishgoit, L.A.; Chernavskii, P.A.; Safonov, V.A.; Filippova, S.E. Magnetic Properties of Electrodeposited Ni–P Alloys with Varying Phosphorus Content. *Russ. J. Phys. Chem.* **2017**, *91*, 260–263. [CrossRef]
7. Knyazev, A.V.; Fishgoit, L.A.; Chernavskii, P.A.; Safonov, V.A.; Filippova, S.E. Magnetic Properties of Electrodeposited Amorphous Nickel–Phosphorus Alloys. *Russ. J. Electrochem.* **2017**, *53*, 270–274. [CrossRef]
8. Liu, S.; Shohji, I.; Kobayashi, T.; Hirohashi, J.; Wake, T.; Yamamoto, H.; Kamakoshi, Y. Mechanistic Study of Ni–Cr–P Alloy Electrodeposition and Characterization of Deposits. *J. Electroanal. Chem.* **2021**, *897*, 115582. [CrossRef]
9. Jiang, W.; Li, H.; Lao, Y.; Li, X.; Fang, M.; Chen, Y. Synthesis and Characterization of Amorphous NiCoP Alloy Films by Magnetic Assisted Jet Electrodeposition. *J. Alloys Compd.* **2022**, *910*, 164848. [CrossRef]
10. Safonov, V.A.; Safonova, O.V.; Fishgoit, L.A.; Kvashnina, K.; Glatzel, P. Chemical State of Phosphorus in Amorphous Ni–Fe–P Electroplates. *Surf. Coat. Technol.* **2015**, *275*, 239–244. [CrossRef]
11. Safonov, V.A.; Fishgoit, L.A.; Safonova, O.V.; Glatzel, P. On the Presence of Covalently Bound Phosphorus in Amorphous Ni–Co–P and Fe–Co–P Electroplates. *Mater. Chem. Phys.* **2021**, *272*, 124987. [CrossRef]
12. Ranjan, P.; Kumar, R.; Walia, R.S. Functionally Graded Material Coatings (FGMC)—A Review. *J. Phys. Conf. Ser.* **2021**, *2007*, 012068. [CrossRef]
13. Moiseev, I.I.; Loktev, A.S.; Shlyakhtin, O.A.; Mazo, G.N.; Dedov, A.G. New Approaches to the Design of Nickel, Cobalt, and Nickel–Cobalt Catalysts for Partial Oxidation and Dry Reforming of Methane to Synthesis Gas. *Pet. Chem.* **2019**, *59*, S1–S20. [CrossRef]

14. Lebedeva, O.; Kultin, D.; Kalmykov, K.; Snytko, V.; Kuznetsova, I.; Orekhov, A.; Zakharov, A.; Kustov, L. Nanorolls Decorated with Nanotubes as a Novel Type of Nanostructures: Fast Anodic Oxidation of Amorphous Fe–Cr–B Alloy in Hydrophobic Ionic Liquid. *ACS Appl. Mater. Interfaces* **2021**, *13*, 2025–2032. [CrossRef] [PubMed]
15. Bernasconi, R.; Panzeri, G.; Accogli, A.; Liberale, F.; Nobili, L.; Magagnin, L. Electrodeposition from Deep Eutectic Solvents. In *Progress and Developments in Ionic Liquids*; Handy, S., Ed.; InTechOpen: London, UK, 2017; ISBN 978-953-51-2901-1.
16. Yamasaki, T. High-Strength Nanocrystalline Ni-W Alloys Produced by Electrodeposition and Their Embrittlement Behaviors during Grain Growth. *Scr. Mater.* **2001**, *44*, 1497–1502. [CrossRef]
17. Quiroga Argañaraz, M.P.; Ribotta, S.B.; Folquer, M.E.; Benítez, G.; Rubert, A.; Gassa, L.M.; Vela, M.E.; Salvarezza, R.C. The Electrochemistry of Nanostructured Ni–W Alloys. *J. Solid State Electrochem.* **2013**, *17*, 307–313. [CrossRef]
18. Wang, Z.; Wu, T.; Geng, X.; Ru, J.; Hua, Y.; Bu, J.; Xue, Y.; Wang, D. The Role of Electrolyte Ratio in Electrodeposition of Nanoscale Fe Cr Alloy from Choline Chloride-Ethylene Glycol Ionic Liquid: A Suitable Layer for Corrosion Resistance. *J. Mol. Liq.* **2022**, *346*, 117059. [CrossRef]
19. Omar, I.M.A.; Al-Fakih, A.M.; Aziz, M.; Emran, K.M. Part II: Impact of Ionic Liquids as Anticorrosives and Additives on Ni-Co Alloy Electrodeposition: Experimental and DFT Study. *Arab. J. Chem.* **2021**, *14*, 102909. [CrossRef]
20. Maizi, R. Electrodeposition of Ni, Fe and Ni-Fe Alloys in Two Ionic Liquids: (Tri (n-Butyl) [2-Methoxy-2-Oxoethyl] Ammonium Bis (Trifluoromethylsulfonyl) [BuGBOEt] [Tf2N] and (1-Butyl-1- Methylpyrrolidinium Bis Trifluoromethylsulfonyl) Imide ([P1,4] [Tf2N]). *Int. J. Electrochem. Sci.* **2016**, *11*, 7111–7124. [CrossRef]
21. Wallace, A.G.; Symes, M.D. Water-Splitting Electrocatalysts Synthesized Using Ionic Liquids. *Trends Chem.* **2019**, *1*, 247–258. [CrossRef]
22. Zhou, J.; Meng, X.; Ouyang, P.; Zhang, R.; Liu, H.; Xu, C.; Liu, Z. Electrochemical Behavior and Electrodeposition of Fe-Co-Ni Thin Films in Choline Chloride/Urea Deep Eutectic Solvent. *J. Electroanal. Chem.* **2022**, *919*, 116516. [CrossRef]
23. Lebedeva, O.; Kultin, D.; Kustov, L. Electrochemical Synthesis of Unique Nanomaterials in Ionic Liquids. *Nanomaterials* **2021**, *11*, 3270. [CrossRef] [PubMed]
24. Lebedeva, O.; Kultin, D.; Zakharov, A.; Kustov, L. Advances in Application of Ionic Liquids: Fabrication of Surface Nanoscale Oxide Structures by Anodization of Metals and Alloys. *Surf. Interfaces* **2022**, *34*, 102345. [CrossRef]
25. Liu, F.; Deng, Y.; Han, X.; Hu, W.; Zhong, C. Electrodeposition of Metals and Alloys from Ionic Liquids. *J. Alloys Compd.* **2016**, *654*, 163–170. [CrossRef]
26. Costa, J.G. dos R. da; Costa, J.M.; Almeida Neto, A.F. de Progress on Electrodeposition of Metals and Alloys Using Ionic Liquids as Electrolytes. *Metals* **2022**, *12*, 2095. [CrossRef]
27. Smith, E.L.; Abbott, A.P.; Ryder, K.S. Deep Eutectic Solvents (DESs) and Their Applications. *Chem. Rev.* **2014**, *114*, 11060–11082. [CrossRef]
28. Brenner, A. *Electrodeposition of Alloys*; Principles and Practice; Academic Press: New York, NY, USA; London, UK, 1963; Volume 1.
29. Landolt, D. Fundamental aspects of alloy plating. *Plat. Surf. Finish.* **2001**, *88*, 70–79.
30. Cao, X.; Wang, H.; Liu, T.; Shi, Y.; Xue, X. Electrodeposition of Bi from Choline Chloride-Malonic Acid Deep Eutectic Solvent. *Materials* **2023**, *16*, 415. [CrossRef]
31. Lv, Q.; Yao, B.; Zhang, W.; She, L.; Ren, W.; Hou, L.; Fautrelle, Y.; Lu, X.; Yu, X.; Li, X. Controlled Direct Electrodeposition of Crystalline NiFe/Amorphous NiFe-(Oxy)Hydroxide on NiMo Alloy as a Highly Efficient Bifunctional Electrocatalyst for Overall Water Splitting. *Chem. Eng. J.* **2022**, *446*, 137420. [CrossRef]
32. Saeki, R.; Yakita, T.; Ohgai, T. Magnetization and Microhardness of Iron–Chromium Alloy Films Electrodeposited from an Aqueous Solution Containing N, N-Dimethylformamide. *J. Mater. Res. Technol.* **2022**, *18*, 2735–2744. [CrossRef]
33. Torabinejad, V.; Aliofkhazraei, M.; Assareh, S.; Allahyarzadeh, M.H.; Rouhaghdam, A.S. Electrodeposition of Ni-Fe Alloys, Composites, and Nano Coatings—A Review. *J. Alloys Compd.* **2017**, *691*, 841–859. [CrossRef]
34. Shetty, A.R.; Hegde, A.C. Effect of Magnetic Field on Corrosion Performance of Ni–Co Alloy Coatings. *J. Bio- Tribo-Corros.* **2023**, *9*, 16. [CrossRef]
35. Haché, M.J.R.; Tam, J.; Erb, U.; Zou, Y. Electrodeposited Nanocrystalline Medium-Entropy Alloys—An Effective Strategy of Producing Stronger and More Stable Nanomaterials. *J. Alloys Compd.* **2022**, *899*, 163233. [CrossRef]
36. Barati Darband, G.; Aliofkhazraei, M.; Rouhaghdam, A.S. Facile Electrodeposition of Ternary Ni-Fe-Co Alloy Nanostructure as a Binder Free, Cost-Effective and Durable Electrocatalyst for High-Performance Overall Water Splitting. *J. Colloid Interface Sci.* **2019**, *547*, 407–420. [CrossRef] [PubMed]
37. Bachvarov, V.; Lefterova, E.; Rashkov, R. Electrodeposited NiFeCo and NiFeCoP Alloy Cathodes for Hydrogen Evolution Reaction in Alkaline Medium. *Int. J. Hydrogen Energy* **2016**, *41*, 12762–12771. [CrossRef]
38. Kothanam, N.; Harachai, K.; Qin, J.; Boonyongmaneerat, Y.; Triroj, N.; Jaroenapibal, P. Hardness and Tribological Properties of Electrodeposited Ni–P Multilayer Coatings Fabricated through a Stirring Time-Controlled Technique. *J. Mater. Res. Technol.* **2022**, *19*, 1884–1896. [CrossRef]
39. Aliofkhazraei, M.; Walsh, F.C.; Zangari, G.; Köçkar, H.; Alper, M.; Rizal, C.; Magagnin, L.; Protsenko, V.; Arunachalam, R.; Rezvanian, A.; et al. Development of Electrodeposited Multilayer Coatings: A Review of Fabrication, Microstructure, Properties and Applications. *Appl. Surf. Sci. Adv.* **2021**, *6*, 100141. [CrossRef]
40. Ma, C.; Wang, S.; Walsh, F.C. The Electrodeposition of Nanocrystalline Cobalt–Nickel–Phosphorus Alloy Coatings: A Review. *Trans. Inst. Met. Finish.* **2015**, *93*, 275–280. [CrossRef]

41. Filgueira de Almeida, A.; Venceslau de Souto, J.I.; Lima dos Santos, M.; Costa de Santana, R.A.; Alves, J.J.N.; Nascimento Campos, A.R.; Prasad, S. Establishing Relationships between Bath Composition and the Properties of Amorphous Ni–Mo Alloys Obtained by Electrodeposition. *J. Alloys Compd.* **2021**, *888*, 161595. [CrossRef]
42. Benavente Llorente, V.; Diaz, L.A.; Lacconi, G.I.; Abuin, G.C.; Franceschini, E.A. Effect of Duty Cycle on NiMo Alloys Prepared by Pulsed Electrodeposition for Hydrogen Evolution Reaction. *J. Alloys Compd.* **2022**, *897*, 163161. [CrossRef]
43. Shojaei, Z.; Khayati, G.R.; Darezereshki, E. Review of Electrodeposition Methods for the Preparation of High-Entropy Alloys. *Int. J. Miner. Metall. Mater.* **2022**, *29*, 1683–1696. [CrossRef]
44. Yue, Z.; Muig, M.; Xiao-Ming, X.; Ze-Lin, L.; Shi-Xun, L.; Sbao-Min, Z. Kinetic Model of Induced Codeposition of Ni-Mo Alloys. *Chin. J. Chem.* **2010**, *18*, 29–34. [CrossRef]
45. Jović, B.M.; Jović, V.D.; Maksimović, V.M.; Pavlović, M.G. Characterization of Electrodeposited Powders of the System Ni–Mo–O. *Electrochim. Acta* **2008**, *53*, 4796–4804. [CrossRef]
46. Podlaha, E.J.; Landolt, D. Induced Codeposition: II. A Mathematical Model Describing the Electrodeposition of Ni-Mo Alloys. *J. Electrochem. Soc.* **1996**, *143*, 893–899. [CrossRef]
47. Manazoğlu, M.; Hapçı, G.; Orhan, G. Electrochemical Deposition and Characterization of Ni-Mo Alloys as Cathode for Alkaline Water Electrolysis. *J. Mater. Eng. Perform.* **2016**, *25*, 130–137. [CrossRef]
48. Tsyntsaru, N.; Cesiulis, H.; Donten, M.; Sort, J.; Pellicer, E.; Podlaha-Murphy, E.J. Modern Trends in Tungsten Alloys Electrodeposition with Iron Group Metals. *Surf. Eng. Appl. Electrochem.* **2012**, *48*, 491–520. [CrossRef]
49. Fishgoit, L.A.; Fedorayev, I.I.; Knyazev, A.V.; Kasyanov, F.V.; Perkovskii, E.A. Electrodeposition of Nanocoatings Involving Iron Triad Metals. *Gal'vanotekh. Obrab. Poverkhn.* **2022**, *30*, 13–28. [CrossRef]
50. Zhu, Z.; Meng, H.; Ren, P. CoNiWReP High Entropy Alloy Coatings Prepared by Pulse Current Electrodeposition from Aqueous Solution. *Colloids Surf. A* **2022**, *648*, 129404. [CrossRef]
51. Zhang, W.; Xia, W.; Li, B.; Li, M.; Hong, M.; Zhang, Z. Influences of Co and Process Parameters on Structure and Corrosion Properties of Nanocrystalline Ni-W-Co Ternary Alloy Film Fabricated by Electrodeposition at Low Current Density. *Surf. Coat. Technol.* **2022**, *439*, 128457. [CrossRef]
52. Crousier, J.; Eyraud, M.; Crousier, J.-P.; Roman, J.-M. Influence of Substrate on the Electrodeposition of Nickel-Molybdenum Alloys. *J. Appl. Electrochem.* **1992**, *22*, 749–755. [CrossRef]
53. Beltowska-Lehman, E.; Chassaing, E. Electrochemical Investigation of the Ni±Cu±Mo Electrodeposition System. *J. Appl. Electrochem.* **1997**, *27*, 568–572. [CrossRef]
54. Allahyarzadeh, M.H.; Aliofkhazraei, M.; Rezvanian, A.R.; Torabinejad, V.; Sabour Rouhaghdam, A.R. Ni-W Electrodeposited Coatings: Characterization, Properties and Applications. *Surf. Coat. Technol.* **2016**, *307*, 978–1010. [CrossRef]
55. Salehikahrizsangi, P.; Raeissi, K.; Karimzadeh, F.; Calabrese, L.; Proverbio, E. Highly Hydrophobic Ni-W Electrodeposited Film with Hierarchical Structure. *Surf. Coat. Technol.* **2018**, *344*, 626–635. [CrossRef]
56. Lee, S.; Choi, M.; Park, S.; Jung, H.; Yoo, B. Mechanical Properties of Electrodeposited Ni-W ThinFilms with Alternate W-Rich and W-Poor Multilayers. *Electrochim. Acta* **2015**, *153*, 225–231. [CrossRef]
57. Slavcheva, E.; Mokwa, W.; Schnakenberg, U. Electrodeposition and Properties of NiW Films for MEMS Application. *Electrochim. Acta* **2005**, *50*, 5573–5580. [CrossRef]
58. Zhang, Z.; Xu, Z.; Liao, Z.; Chen, C.; Wei, G. A Novel Synthesis Method for Functionally Graded Alloy Coatings by Induced Electrodeposition. *Mater. Lett.* **2022**, *312*, 131681. [CrossRef]
59. Zhang, Z.; Dai, L.; Yin, Y.; Xu, Z.; Lv, Y.; Liao, Z.; Wei, G.; Zhong, F.; Yuan, M. Electrodeposition and Wear Behavior of NiCoW Ternary Alloy Coatings Reinforced by Al_2O_3 Nanoparticles: Influence of Current Density and Electrolyte Composition. *Surf. Coat. Technol.* **2022**, *431*, 128030. [CrossRef]
60. Cesiulis, H.; Tsyntsaru, N.; Budreika, A.; Skridaila, N. Electrodeposition of CoMo and CoMoP Alloys from the Weakly Acidic Solutions. *Surf. Eng. Appl. Electrochem.* **2010**, *46*, 406–415. [CrossRef]
61. Huang, H.; Hu, X.; Zhang, J.; Su, N.; Cheng, J. Facile Fabrication of Platinum-Cobalt Alloy Nanoparticles with Enhanced Electrocatalytic Activity for a Methanol Oxidation Reaction. *Sci. Rep.* **2017**, *7*, 45555. [CrossRef]
62. Saito, G.; Akiyama, T. Nanomaterial Synthesis Using Plasma Generation in Liquid. *J. Nanomater.* **2015**, *16*, 299. [CrossRef]
63. Endres, F.; Abbott, A.; MacFarlane, D. (Eds.) *Electrodeposition from Ionic Liquids*, 2nd ed.; Wiley-VCH Verlag GmbH & Co. KGaA: Weinheim, Germany, 2017; ISBN 978-3-527-68270-6.
64. Greer, A.J.; Jacquemin, J.; Hardacre, C. Industrial Applications of Ionic Liquids. *Molecules* **2020**, *25*, 5207. [CrossRef] [PubMed]
65. Ispas, A.; Bund, A. Electrodeposition in Ionic Liquids. *Electrochem. Soc. Interface* **2014**, *23*, 47–51. [CrossRef]
66. Omar, I.M.A.; Aziz, M.; Emran, K.M. Part I: Ni-Co Alloy Foils Electrodeposited Using Ionic Liquids. *Arab. J. Chem.* **2020**, *13*, 7707–7719. [CrossRef]
67. Mohanty, U.S.; Tripathy, B.C.; Singh, P.; Keshavarz, A.; Iglauer, S. Roles of Organic and Inorganic Additives on the Surface Quality, Morphology, and Polarization Behavior during Nickel Electrodeposition from Various Baths: A Review. *J. Appl. Electrochem.* **2019**, *49*, 847–870. [CrossRef]
68. Danilov, F.I.; Bogdanov, D.A.; Smyrnova, O.V.; Korniy, S.A.; Protsenko, V.S. Electrodeposition of Ni–Fe Alloy from a Choline Chloride-Containing Ionic Liquid. *J. Solid State Electrochem.* **2022**, *26*, 939–957. [CrossRef]
69. Tułodziecki, M.; Tarascon, J.-M.; Taberna, P.L.; Guéry, C. Importance of the Double Layer Structure in the Electrochemical Deposition of Co from Soluble Co2+—Based Precursors in Ionic Liquid Media. *Electrochim. Acta* **2014**, *134*, 55–66. [CrossRef]

70. Brenner, A. *Electrodeposition of Alloys. 2: Practical and Specific Information*; Academic Press: New York, NY, USA, 1963; ISBN 978-1-4832-0967-8.
71. Abbott, A.P. Deep Eutectic Solvents and Their Application in Electrochemistry. *Curr. Opin. Green Sustain. Chem.* **2022**, *36*, 100649. [CrossRef]
72. Smith, E.L. Deep Eutectic Solvents (DESs) and the Metal Finishing Industry: Where Are They Now? *Trans. Inst. Met. Finish.* **2013**, *91*, 241–248. [CrossRef]
73. Gómez, E.; Fons, A.; Cestaro, R.; Serrà, A. Electrodeposition of CoNi Alloys in a Biocompatible DES and Its Suitability for Activating the Formation of Sulfate Radicals. *Electrochim. Acta* **2022**, *435*, 141428. [CrossRef]
74. Landa-Castro, M.; Sebastián, P.; Giannotti, M.I.; Serrà, A.; Gómez, E. Electrodeposition of Nanostructured Cobalt Films from a Deep Eutectic Solvent: Influence of the Substrate and Deposition Potential Range. *Electrochim. Acta* **2020**, *359*, 136928. [CrossRef]
75. Oliveira, F.G.S.; Santos, L.P.M.; da Silva, R.B.; Correa, M.A.; Bohn, F.; Correia, A.N.; Vieira, L.; Vasconcelos, I.F.; de Lima-Neto, P. FexNi(1-x) Coatings Electrodeposited from Choline Chloride-Urea Mixture: Magnetic and Electrocatalytic Properties for Water Electrolysis. *Mater. Chem. Phys.* **2022**, *279*, 125738. [CrossRef]
76. Higashino, S.; Abbott, A.P.; Miyake, M.; Hirato, T. Iron(III) Chloride and Acetamide Eutectic for the Electrodeposition of Iron and Iron Based Alloys. *Electrochim. Acta* **2020**, *351*, 136414. [CrossRef]
77. Niciejewska, A.; Ajmal, A.; Pawlyta, M.; Marczewski, M.; Winiarski, J. Electrodeposition of Ni–Mo Alloy Coatings from Choline Chloride and Propylene Glycol Deep Eutectic Solvent Plating Bath. *Sci. Rep.* **2022**, *12*, 18531. [CrossRef] [PubMed]
78. Ysea, N.B.; Benavente Llorente, V.; Loiácono, A.; Lagucik Marquez, L.; Diaz, L.; Lacconi, G.I.; Franceschini, E.A. Critical Insights from Alloys and Composites of Ni-Based Electrocatalysts for HER on NaCl Electrolyte. *J. Alloys Compd.* **2022**, *915*, 165352. [CrossRef]
79. You, Y.; Gu, C.; Wang, X.; Tu, J. Electrochemical Synthesis and Characterization of Ni–P Alloy Coatings from Eutectic–Based Ionic Liquid. *J. Electrochem. Soc.* **2012**, *159*, D642–D648. [CrossRef]